Intracavity cold atomic ensemble with high optical depth

View Online   Export Citation   CrossMark

Yue Jiang, Yefeng Mei, [ID] Yueyang Zou, Ying Zuo, [ID] and Shengwang Du[a] [ID]

AFFILIATIONS

Department of Physics, The Hong Kong University of Science and Technology, Clear Water Bay, Kowloon, Hong Kong, China

[a]Electronic mail: dusw@ust.hk

ABSTRACT

We describe the apparatus of an optical cavity loaded with cold ^{85}Rb atoms of high optical depth (OD) in the weak coupling regime. The relevant cavity-atom parameters are the single-photon Rabi frequency $g_0 = 2\pi \times 0.25$ MHz, the cavity power decay rate $\kappa = 2\pi \times 9.0$ MHz, and the atomic excited state decay rate $\Gamma = 2\pi \times 5.75$ MHz. In this bad-cavity configuration where the atomic natural linewidth ($\Gamma/2\pi$) is less than the cavity linewidth ($\kappa/2\pi$), the cavity enhancement factor for the longitudinal OD is about 188. We obtain a cavity enhanced OD up to 7600, corresponding to an atomic ensemble with a bare single-pass OD of 40, coupled to the cavity mode. Our intracavity cold atomic ensemble with high OD may have many applications in studying collective atom-light interaction inside an optical cavity.

Published under license by AIP Publishing. https://doi.org/10.1063/1.5065431

I. INTRODUCTION

Strong atom-light interaction is crucial in many quantum applications involving atoms and photons. In free space, collective enhancement can be achieved using a dense atomic cloud, where the optical depth OD = $n\sigma L$ is an important measure. Here n is the atomic density, σ is the absorption cross section, and L is the sample length. For example, in an optical quantum memory, the storage efficiency depends strongly on the OD.[1-3] Many techniques have been developed for achieving high OD with laser-cooled atoms, such as increasing L with two-dimensional (2D) magneto-optical trap (MOT),[4-6] enhancing the atomic density n by spatial dark-line[6] and temporal dark spot,[7] or optimizing σ by optically pumping atoms to a certain Zeeman-state with a large Clebsch-Gordan coefficient.[8] With all these efforts, so far the highest OD record in free space is 1306 but with the sacrifice of the low repetition rate (7.5 Hz) and the duty cycle (0.1%).[9] Obtaining a higher OD in free space remains a challenge.

An alternative approach to enhance the atom-light interaction is loading the atoms into an optical cavity, where a photon can have many round trips inside the cavity before it leaks out such that the cavity enhanced OD (OD_c) can be many times of that (OD_0) in free space. However, to directly trap highly dense cold atoms inside an optical cavity is technically difficult because efficient laser cooling and trapping requires a large free-space volume which is not compatible to the cavity setup. Therefore, most atom-cavity systems are operated in the strong-coupling regime with modest bare OD ($OD_0 < 10$)[10,11] and even single atoms,[12-16] where the atom-light interaction is enhanced mainly because of the intracavity photon confinement. In these systems, the cavity linewidth is much narrower than the atomic natural linewidth such that the output is extremely sensitive to the stability of the cavity alignment.

Recently, the bad-cavity configuration, where the atomic natural linewidth is less than the cavity linewidth, attracted much research interests because of its cavity-alignment insensitivity and application in producing a superradiant laser with very few intracavity photons.[17] In this intermediate regime, both atomic collective enhancement and cavity photon confinement play important roles.

In this paper, we describe a cold-atom cavity apparatus in the bad-cavity configuration with an ultrahigh effective optical depth. Making use of a dark-line 2D MOT embedded inside an optical cavity, we trapped a line of cold atoms with an OD_c as high as 7600, which corresponds to a cavity enhancement

of 188 as compared to its bare single-path OD of 40. Compared to other atom-cavity systems with modest bare OD ($OD_0 < 10$), our system is unique. It will have important applications in studying cavity quantum electrodynamics (QED) in the weak coupling regime, where the coherence is mainly determined by the atoms instead of the cavity parameters, while in the strong coupling regime, the narrow cavity resonance drives the system coherence.
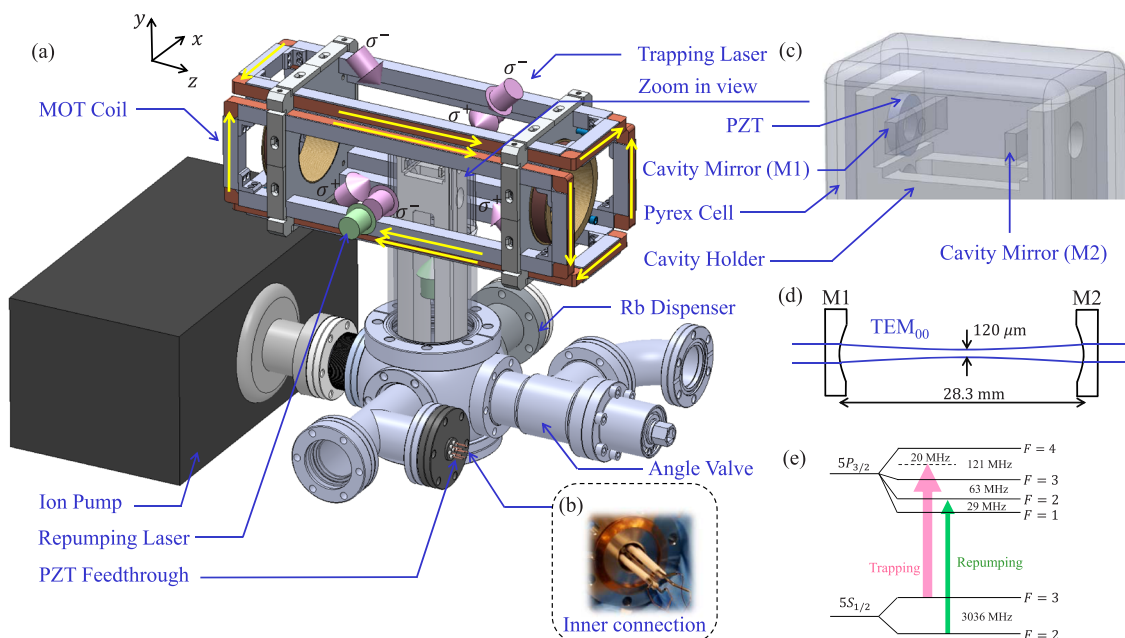
II. OPTICAL CAVITY AND 2D MOT SETUP

The core part of our atom-cavity apparatus is a dark-line 2D MOT inside an optical cavity, and the whole setup is put inside an ultra-high vacuum (UHV) chamber, as shown in Fig. 1(a). A six-way cross (MCF450-SphSq-E2C4, Kimball Physics, Inc.) is used to connect and mount all the parts. The MOT chamber is a Pyrex glass cell (without coating, customized from Precision Glassblowing, Inc.). A bias tee (T-0275, Kurt J. Lesker Company) connects the piezoelectric transducer (PZT) feed-through (EFT0081033, Kimball Physics, Inc.). The inner connections of Kapton coated PZT wires and PZT feed-through are shown in Fig. 1(b), where the PZT wires are connected by 1 mm inner diameter capillary tubes to the feed-through. To avoid possible corrosion caused by Rb atoms, the Rb dispensers (SAES, RB/NF/4.8/17 FT10 + 10) are mounted on the opposite port to PZT feed-through. We spot welded total seven Rb dispensers to dispenser feed-through (1014301, MDC vacuum products, LLC.). By changing the dispenser current, we can vary the Rb vapor pressure from 10^{-10} to 10^{-7} Torr.

For the experiments described in this paper, we use only two of the Rb dispensers, and the other five are remained off.

A. Optical cavity

We work with a near confocal standing-wave cavity, which comprises of a cavity holder (customized by Michan), two Piezos (PZT, APC, HPCh 150/15-8/3), and two cavity mirrors (customized by CASIX, Inc.). To minimize cavity length change caused by temperature fluctuation (mainly caused by heating from the Rb dispensers), the cavity holder is made of low thermal expansion material Zerodur. Torr Seal (Agilent, Torr seal 9530001) is used to glue the PZTs to the cavity holder and cavity mirrors to PZTs. The cavity length can be finely tuned by the two PZTs (26 μm/V). The geometry of the cavity mirror alignment is shown in the zoomed-in view of the optical cavity inside the Pyrex cell in Fig. 1(c), whose fused silica substrates have the same size of 30 mm × 8 mm and a thickness of 2.92 mm. The curved area, with a curvature of 30 mm and a diameter of 4 mm, is located at the center of the rectangular mirror. These geometries are designed to allow a large MOT trapping volume and maximize the optical access. Both curved and plane areas of the front surface have high-reflection coating. The two cavity mirrors are designed to have different power reflectivity at 795 nm optical wavelength: $R_1 = 99.975\%$ for M1 and $R_2 = 98.973\%$ for M2. The cavity length is $L_c = 28.3$ mm, locked to a reference laser injected to the TEM_{00} mode of the cavity, as shown in Fig. 1(d). We use the Pound-Drever-Hall technique to lock the cavity length. We dither reference laser's frequency by an acousto-optic

FIG. 1. (a) System overview of the atom-cavity apparatus with the 2D MOT setup. (b) The inner connection of PZT feed-through. (c) The zoomed-in view of the optical cavity inside the Pyrex cell. (d) Schematics of the optical cavity with mirrors M1 and M2 in the presence of a TEM_{00} Gaussian mode beam. (e) Atomic energy level diagram of ^{85}Rb D2 line for laser cooling and trapping.

modulator and couple it to cavity TEM_{00} mode. The transmission spectrum is collected by a photodiode so that the cavity can be locked to the transmission peak with the standard proportional-integral-derivative loop controller. The reference laser is beating, locked to a master reference 795 nm laser. In this way, we have a large frequency tuning range to lock the cavity. The measured free spectral range (FSR) is 5.262 GHz and cavity linewidth $\kappa = 2\pi \times 9.0$ MHz. The finesse $\mathcal{F} = 2\pi$ FSR$/\kappa = 590$ is consistent with the designed value $\mathcal{F} = \pi(R_1 R_2)^{1/4}/(1 - \sqrt{R_1 R_2}) = 594$.

For Rb D1 line transitions (795 nm), the atomic spontaneous decay rate of the excited states is $\Gamma = 2\pi \times 5.75$ MHz. The single-photon-induced cavity Rabi frequency is determined by $g_0 \equiv \frac{\mu}{\hbar}\sqrt{\frac{\hbar\omega_c}{2\epsilon_0 V_m}}$, where μ is the atomic dipole moment, ω_c is the resonance frequency of the cavity, and V_m is the cavity mode volume. In our system, we have $g_0 = 2\pi \times 0.25$ MHz. Following the criterion $g_0/(\Gamma, \kappa) \ll 1$,[18] we verify that our atom-cavity system is in the weak coupling regime.

B. Dark-line 2D MOT

A typical dark-line 2D ^{85}Rb MOT setup consists of a 2D quadrupole magnetic field, trapping beams from six directions and two repumping beams.[6] As illustrated in Fig. 1(a), the quadrupole magnetic field is generated by four packs of 100 turns copper wires mounted on the aluminum frames. To avoid induced eddy current, the turning ends of the aluminum frames are insulated by Kapton tape and the connecting screws are made of Teflon. These water-cooled-free coils generate 10 G/cm radial 2D magnetic field gradient on the transverse plane at an operating current of 2.8 A. The magnetic field gradient is zero along the longitudinal axis. The ^{85}Rb atomic energy levels involved in trapping and repumping are plotted in Fig. 1(e): the trapping laser is 20 MHz red detuned from the transition $|5S_{1/2}, F = 3\rangle \rightarrow |5P_{3/2}, F = 4\rangle$, and the repumping laser is on resonance to the transition $|5S_{1/2}, F = 2\rangle \rightarrow |5P_{3/2}, F = 2\rangle$. The six trapping beams shown in Fig. 1(a) are indicated with pink arrows. The diameter of the trapping beams at $1/e^2$ intensity is 15 mm, which is limited by the geometry of the Zerodur cavity holder. We align two of the trapping beams along x and -x directions, while the other four are aligned at 45° angles to the y and z axes. In this way, the optical access along the z direction is fully opened and does not interfere with the trapping laser beams. With the illustrated magnetic coil current direction and magnetic field, the polarizations (σ^+ and σ^-) of the six trapping beams are also shown in Fig. 1(a). We use two repumping laser beams (marked with green arrows) to pump the atoms in $|5S_{1/2}, F = 2\rangle$ to $|5S_{1/2}, F = 3\rangle$ and keep them in the cooling cycles. The atoms are trapped along the longitudinal z axis of the cavity to obtain the maximum OD. To have the dark-line MOT, one of the repumping beams overlaps with the trapping beam along the x axis, and the other repumping beam is aligned along the y axis. There is a copper wire line with a diameter of 0.7 mm in each repumping beam optical path. The images of these copper wires with a unit magnification, through a 4f lens system in each beam, are projected at the center of the 2D MOT to create a repumping dark line
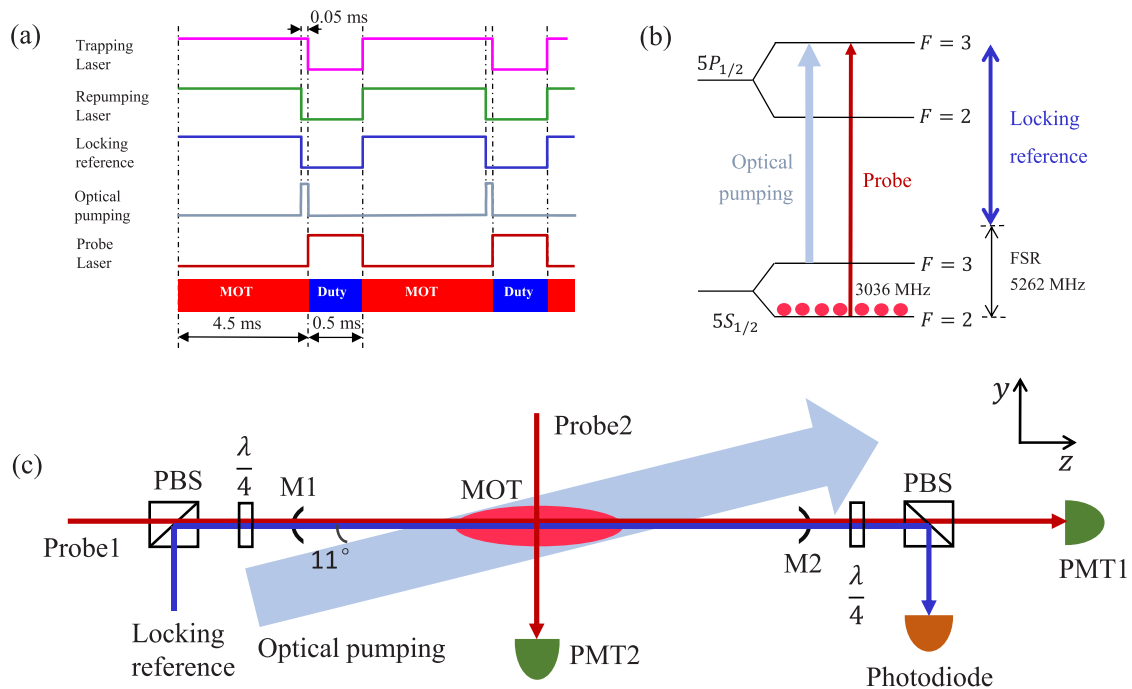
FIG. 2. OD measurement scheme. (a) Experimental timing cycles. (b) Atomic energy level diagram of ^{85}Rb D1 line. (c) Optical setup for OD measurement.

(with a square cross section of 0.7×0.7 mm^2) along the z axis. In the dark line regime, the atoms are pumped into the dark state $|5S_{1/2}, F = 2\rangle$ without interacting with the trapping laser and thus avoid the radiation trapping loss and heating. The dark-line configuration increases OD by 30% in our system.

III. OD MEASUREMENT AND CHARACTERIZATION

To characterize the cavity enhancement on the atom-light interaction, we take a measure of the cavity enhanced OD. The experiment is run periodically with the period T = 5 ms, including the MOT time t_{MOT} = 4.5 ms followed by measurement duty time t_{duty} = 0.5 ms, as shown in Fig. 2(a). The duty cycle $\eta = t_{duty}/T$ is 10%. At each cycle, to the end of the MOT time, we switch off the repumping laser and leave the trapping laser on for additional 50 μs to optically pump atoms into the ground state $|5S_{1/2}, F = 2\rangle$. To ensure that all the atoms are pumped, during that 50 μs time we apply an additional optical pumping beam on resonance to the transition $|5S_{1/2}, F = 3\rangle$ to $|5P_{1/2}, F = 3\rangle$, as shown in Fig. 2(b). The optical pumping beam has a collimated $1/e^2$ beam diameter of 4 mm and is aligned at 11° to the z direction, as shown in Fig. 2(c). In our experiment, the optical pumping beam improves the pumping effect because of the ineffective optical pumping of the red-detuned trapping laser beams. We switch on the probe laser beam (Probe1) for transmission measurement inside the duty window. The probe transmission signal is recorded by a photomultiplier tube (PMT1).

The empty cavity resonance is locked to the OD probe transition $|5S_{1/2}, F = 2\rangle \rightarrow |5P_{1/2}, F = 3\rangle$ by setting the reference laser frequency red detuned one FSR from the resonance, as shown in Fig. 2(b). The measurement optical setup is illustrated in Fig. 2(c), where a weak probe laser beam (Probe1) is coupled to cavity TEM$_{00}$ mode through high reflectivity mirror M1, propagating along the 2D MOT longitudinal z axis and is focused to the center of MOT with a $1/e^2$ beam diameter of 120 μm at the waist. The probe laser beam is circularly polarized (σ^+). We collect the probe light through the low reflectivity mirror (M2) to a single mode fiber and passing a 25 dB broadband Fabry-Perot (FP) filter to filter out locking laser leakage and then sent to PMT1. By scanning its frequency across the transition $|5S_{1/2}, F = 2\rangle$ to $|5P_{1/2}, F = 3\rangle$, we get the probe transmission spectrum. The probe laser transition pumps the atoms from $|5S_{1/2}, F = 2\rangle$ to $|5S_{1/2}, F = 3\rangle$. To ensure that the pump effect caused by the probe beam is negligible, we keep the intensity of the probe laser beam sufficiently low ($<8.8 \times 10^{-4}$ nW/cm^2) in cavity so that the atomic population remains primarily in the ground state $|5S_{1/2}, F = 2\rangle$. The bandwidth of the probe laser is about 100 kHz, which is much narrower than the natural linewidth of about 6 MHz of Rb D1 and D2 lines.

In principle with the known finesse $\mathcal{F}$, we can determine the cavity-enhanced OD (OD$_c$) by[19]

$$\mathrm{OD}_c = \frac{\mathcal{F}}{\pi}\mathrm{OD}_0, \qquad (1)$$

where OD$_0$ is the free-space single-pass bare OD. However, we are not able to directly measure OD$_0$ in the presence of the cavity. Figure 3(a) shows typical transmission measurements of the cavity. The black squares are measured for the empty cavity without atoms, whose linewidth is $\kappa/(2\pi)$ = 9.0 MHz. As we load atoms to the cavity, the cavity resonance peak splits into two with a frequency separation of $\Omega/(2\pi)$, which is called the vacuum Rabi splitting (VRS). The VRS strongly depends on the cavity-enhanced OD as[20]

$$\Omega = \sqrt{\mathrm{OD}_c \kappa \Gamma}. \qquad (2)$$

Therefore by measuring the VRS, we can get $\mathrm{OD}_c = \frac{\Omega^2}{\kappa\Gamma}$ and $\mathrm{OD}_0 = \frac{\pi\Omega^2}{\mathcal{F}\kappa\Gamma}$. Figure 3(b) shows our measured VRS up to 627 MHz, which corresponds to OD$_c$ = 7600 and OD$_0$ = 40.

The bare OD can also be determined by measuring the transverse OD of the 2D MOT and its aspect ratio. Because the transverse directions are open to free space, the transverse OD can be measured directly by a second probe beam (Probe2) shown in Fig. 2(c), detected by PMT2. We take a measurement at VRS of 350 MHz and obtain the transverse optical depth OD$_t$ = 1.2. To determine the 2D MOT aspect ratio,
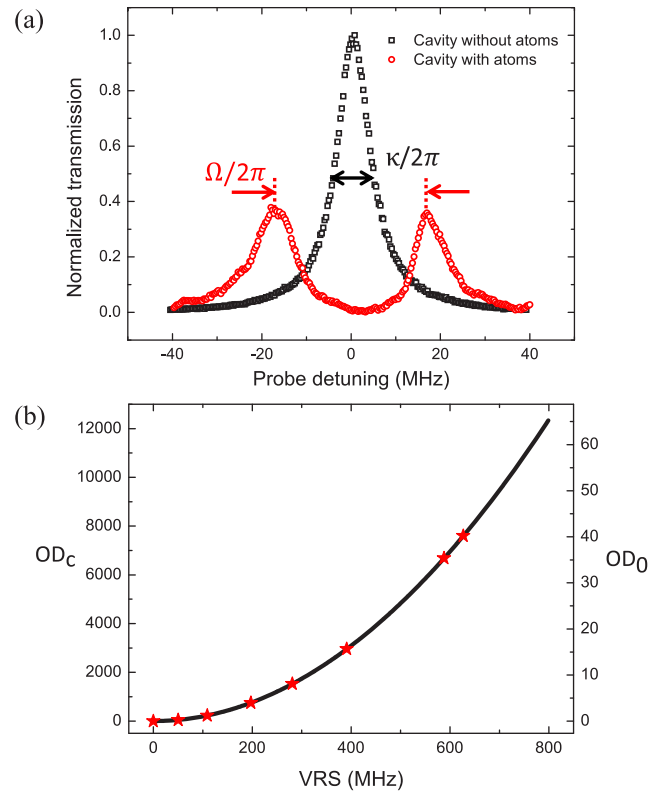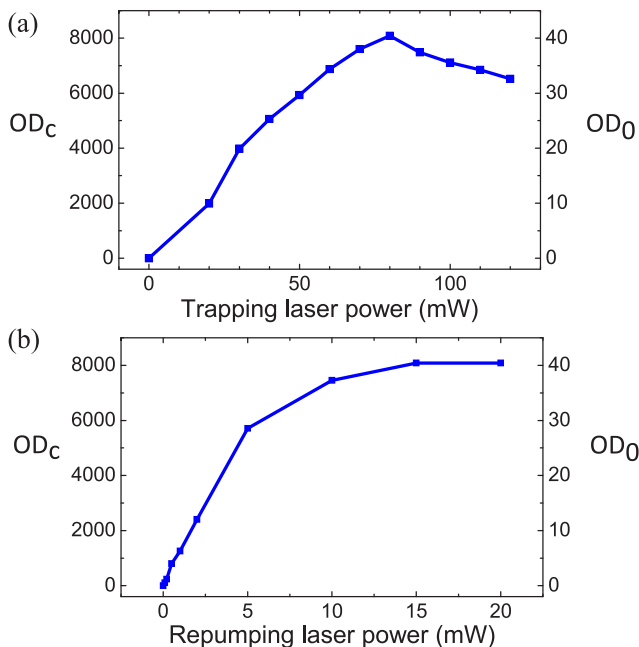

FIG. 3. OD measurement with vacuum Rabi splitting (VRS). (a) Cavity transmission with and without atoms. The black squares are the measured data for cavity transmission without atoms, showing a full width at half maximum (FWHM) $\kappa/2\pi$ = 9.0 MHz. The red circle is measured in presence of cold atoms, showing a VRS $\Omega/2\pi$ = 34 MHz. (b) OD vs VRS.
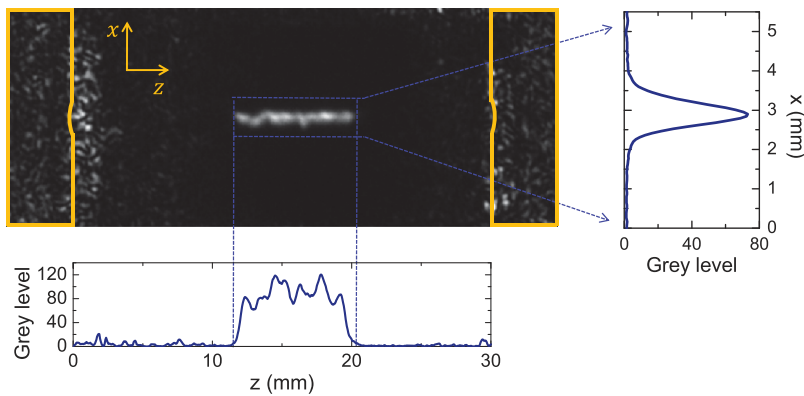
FIG. 4. Fluorescence image of the cold atoms in the 2D MOT. The yellow line indicates the cavity mirror location. The grey level gives the relative intensity of the atoms fluorescence. The grey level data plotted in the bottom are obtained by averaging 20 rows' grey level of the MOT central part. The grey level data plotted in the right side are obtained by averaging 300 columns' grey level of the MOT central part.

we take a fluorescence image as shown in Fig. 4, from which we get its longitudinal length $L = 8$ mm and the effective transverse width $d = 0.68$ mm. Then the aspect ratio of the 2D MOT is about 11.7. We thus obtain the longitudinal bare optical depth $OD_0 = OD_t \times L/d = 14.1$, which is consistent with the value 12.6 (within measurement fluctuation) obtained from Eqs. (1) and (2) with the measured VRS. Therefore, we validate that the VRS measurement is reliable for determining the atom-cavity parameters.

Now we turn to the optimization of the intracavity cold atom loading according to the trapping and repumping laser powers. Figure 5 shows the measured OD (OD_c and OD_0) as a function of the trapping and repumping laser powers at the

fixed dispenser current of 3.5 A. The highest OD is achieved at the trapping laser power of 80 mW [Fig. 5(a)], and it saturates as the repumping laser power is more than 10 mW [Fig. 5(b)].

The number of atoms loaded into the cavity can also be controlled by adjusting the dispenser current. In Fig. 6, we plot the dependence of the measured OD on the current of two dispensers in series. The OD increases exponentially as we increase the dispenser current. The threshold current is about 2.5 A. We obtain $OD_c = 7600$ at 3.5 A.

In the above measurements, we take the duty cycle at 10%. We can vary the MOT loading time to change the duty cycle, while the measurement duty time is fixed at 0.5 ms. During the duty measurement time window, there is atom number loss resulting from the collision with the background residual room-temperature atoms and molecules. As a result, atomic OD varies as a function of the duty cycle. Figure 7 shows the measured OD as a function of the duty cycle at the dispenser current of 3.5 A, with the trapping and repumping laser powers at 80 mW and 20 mW, respectively. The optimal $OD_c = 7600$ is obtained at $\eta = 10\%$. As we increase the duty cycle to 50%, the OD_c drops to about 3000. For some experiments requiring a high OD, we can operate the system with a small duty cycle for longer data-collecting time; otherwise, we operate

FIG. 5. The measured OD as a function of the trapping and repumping powers at a fixed dispenser current of 3.5 A. (a) The repumping laser power is fixed at 20 mW. (b) The trapping laser power is fixed at 80 mW.
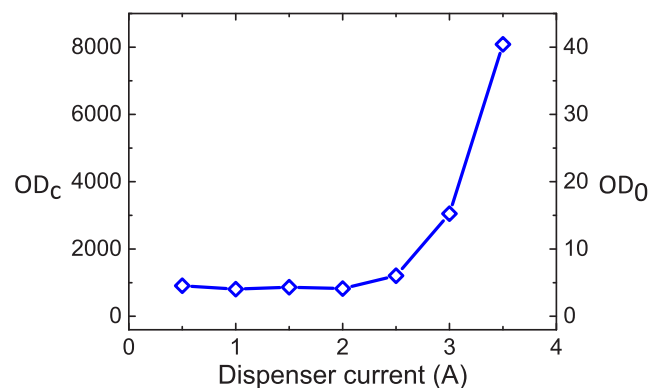
FIG. 6. The measured OD as a function of the current of two dispensers in series. The trapping and repumping powers are 80 mW and 20 mW, respectively.
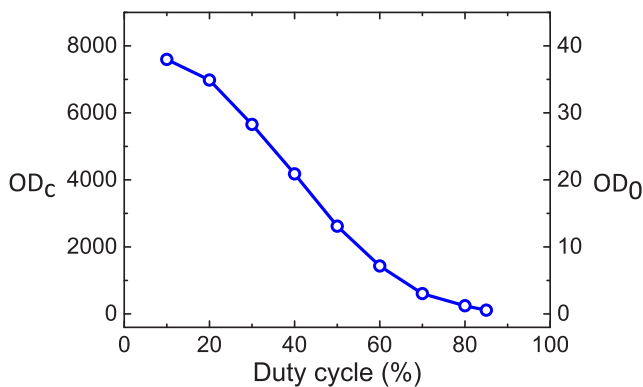
FIG. 7. The measured OD as a function of the duty cycle. The dispenser current is 3.5 A. The trapping and repumping powers are 80 mW and 20 mW, respectively.

the system with a higher duty cycle for a modest OD. Our apparatus is designed for studying cavity QED, particularly for the quantum interactions between atoms and single photons inside the cavity. Such kind of experiments (e.g., narrowband biphoton generation[23–25]) normally require collecting data for many repeated cycles to build the statistics, and a small duty cycle leads to a long data collecting time. In the case where only a high OD is considered, we can achieve a much higher OD_c (>10 000) in our system by adding additional cooling processes [such as compressed MOT (CMOT), polarization gradient cooling (PGC), and even evaporative cooling] with the cost of ultra-small duty cycle. Therefore, we take the product of the cavity enhanced OD_c and the duty cycle to define the figure of merit (FOM) of the system. FOM describes the average OD or the system usage efficiency, providing a measure for designing an experiment with a balanced OD and duty cycle. In our apparatus, the maximum FOM is 1697, obtained at a duty cycle of 30% and OD_c = 5657.

IV. SUMMARY

In summary, we have demonstrated trapping cold ^{85}Rb atoms with high OD inside an optical cavity with the bad-cavity configuration in the weak-coupling regime. Under the 10% duty cycle, we obtain a cavity enhanced OD_c as high as 7600, which corresponds to a cavity enhancement factor of about 188. The high OD_c-duty cycle product (up to 1697) is one of the advantages of our system compared to other atom-cavity apparatus reported. We must mention that in the experiment described in this paper, the probe laser is on an open transition $|5S_{1/2}, F = 2\rangle \rightarrow |5P_{1/2}, F = 3\rangle$ with an absorption cross section σ = 7.82×10^{-14} m^2. This open transition can be used for many quantum optics applications, such as electromagnetically induced transparency,[21] four-wave mixing,[22] and photon pair generation.[23–25] At OD_c = 7600, the single-pass OD_0 = 40, which corresponds to an atomic density-length product $nL = 5.12 \times 10^{14}$ m^{-2} and a total atom number of about 2.0×10^8. In a closed two-state system with $\sigma_{closed} = 3\lambda^2/(2\pi) = 3.02 \times 10^{-13}$ m^2, we can get OD_c more than 29 300. A much higher OD_c in our system can also

be achieved by adding additional cooling processes (such as CMOT, PGC, and evaporative cooling) but with the cost of ultra-small duty cycle. Our apparatus provides a new platform for studying collective atom-light interaction inside an optical cavity.

REFERENCES

[1]S. Zhang, S. Zhou, M. Loy, G. K. L. Wong, and S. Du, "Optical storage with electromagnetically induced transparency in a dense cold atomic ensemble," Opt. Lett. **36**, 4530 (2011).

[2]A. V. Gorshkov, A. Ande, M. Fleischhauer, A. S. Sorensen, and M. D. Lukin, "Universal approach to optimal photon storage in atomic media," Phys. Rev. Lett. **98**, 123601 (2007).

[3]Y.-H. Chen, M.-J. Lee, W. I-Chung, S. Du, Y.-F. Chen, Y.-C. Chen, and I. A. Yu, "Coherent optical memory with high storage efficiency and large fractional delay," Phys. Rev. Lett. **110**, 083601 (2013).

[4]E. Riis, D. S. Weiss, K. A. Moler, and S. Chu, "Atom funnel for the production of a slow, high-density atomic beam," Phys. Rev. Lett. **64**, 1658–1661 (1990).

[5]K. Dieckmann, R. J. C. Spreeuw, M. Weidemüller, and J. T. M. Walraven, "Two-dimensional magneto-optical trap as a source of slow atoms," Phys. Rev. A **58**, 3891–3895 (1998).

[6]S. Zhang, J. Chen, C. Liu, S. Zhou, M. Loy, G. K. L. Wong, and S. Du, "A dark-line two-dimensional magneto-optical trap of 85Rb atoms with high optical depth," Rev. Sci. Instrum. **83**, 073102 (2012).

[7]M. T. DePue, S. L. Winoto, D. Han, and D. S. Weiss, "Transient compression of a mot and high intensity fluorescent imaging of optically thick clouds of atoms," Opt. Commun. **180**, 73–79 (2000).

[8]Y.-F. Hsiao, P.-J. Tsai, H.-S. Chen, S.-X. Lin, C.-C. Hung, C.-H. Lee, Y.-H. Chen, Y.-F. Chen, I. A. Yu, and Y.-C. Chen, "Highly efficient coherent optical memory based on electromagnetically induced transparency," Phys. Rev. Lett. **120**, 183602 (2018).

[9]Y.-F. Hsiao, H.-S. Chen, P.-J. Tsai, and Y.-C. Chen, "Cold atomic media with ultrahigh optical depths," Phys. Rev. A **90**, 055401 (2014).

[10]W. Chen, K. M. Beck, R. Bücker, M. Gullans, M. D. Lukin, H. Tanji-Suzuki, and V. Vuletić, "All-optical switch and transistor gated by one stored photon," Science **341**, 768 (2013).

[11]T. Tiecke, J. D. Thompson, N. P. de Leon, L. Liu, V. Vuletić, and M. D. Lukin, "Nanophotonic quantum phase switch with a single atom," Nature **508**, 241 (2014).

[12]S. Haroche, "Nobel lecture: Controlling photons in a box and exploring the quantum to classical boundary," Rev. Mod. Phys. **85**, 1083 (2013).

[13]D. Meschede, H. Walther, and G. Müller, "One-atom maser," Phys. Rev. Lett. **54**, 551 (1985).

[14]C. Hood, M. Chapman, T. Lynn, and H. Kimble, "Real-time cavity QED with single atoms," Phys. Rev. Lett. **80**, 4157 (1998).

[15]S. Gleyzes, S. Kuhr, C. Guerlin, J. Bernu, S. Deleglise, U. B. Hoff, M. Brune, J.-M. Raimond, and S. Haroche, "Quantum jumps of light recording the birth and death of a photon in a cavity," Nature **446**, 297 (2007).

[16]C. Guerlin, J. Bernu, S. Deleglise, C. Sayrin, S. Gleyzes, S. Kuhr, M. Brune, J.-M. Raimond, and S. Haroche, "Progressive field-state collapse and quantum non-demolition photon counting," Nature **448**, 889 (2007).

[17]J. G. Bohnet, Z. Chen, J. M. Weiner, D. Meiser, M. J. Holland, and J. K. Thompson, "A steady-state superradiant laser with less than one intracavity photon," Nature **484**, 78 (2012).

[18]H. J. Kimble, "Strong interactions of single atoms and photons in cavity QED," Phys. Scr. **T76**, 127 (1998).

[19] H. Tanji, *Few-Photon Nonlinearity with an Atomic Ensemble in an Optical Cavity* (Harvard University, 2011).

[20] J. Simon, *Cavity QED with Atomic Ensembles* (Harvard University, 2010).

[21] K.-J. Boller, A. Imamoğlu, and S. E. Harris, "Observation of electromagnetically induced transparency," Phys. Rev. Lett. **66**, 2593 (1991).

[22] D. A. Braje, V. Balić, S. Goda, G. Yin, and S. Harris, "Frequency mixing using electromagnetically induced transparency in cold atoms," Phys. Rev. Lett. **93**, 183601 (2004).

[23] V. Balić, D. A. Braje, P. Kolchin, G. Yin, and S. E. Harris, "Generation of paired photons with controllable waveforms," Phys. Rev. Lett. **94**, 183601 (2005).

[24] S. Du, J. Wen, and M. H. Rubin, "Narrowband biphoton generation near atomic resonance," J. Opt. Soc. Am. B **25**, C98–C108 (2008).

[25] L. Zhao, X. Guo, C. Liu, Y. Sun, M. M. T. Loy, and S. Du, "Photon pairs with coherence time exceeding 1 μs," Optica **1**, 84–88 (2014).